The copper ionophore disulfiram improves mitochondrial function in various yeast and human cellular models of mitochondrial diseases

Claire Almyre, Nolwenn Bounaix, François Godard, Olivier Baris, Anne-Louise Cayer, Elodie Sardin, Marine Bouhier, Anaïs Hoarau, Laetitia Dard, Jérémy Richard, et al.

The copper ionophore disulfiram improves mitochondrial function in various yeast and human cellular models of mitochondrial diseases

Claire Almyre[1,§], Nolwenn Bounaix[2,§], François Godard[1,§], Olivier R. Baris[2], Anne-Louise Cayer[1], Elodie Sardin[1], Marine Bouhier[1], Anaïs Hoarau[1], Laetitia Dard[1], Jérémy Richard[2], Vanessa Bergeron[1], Aurélie Renaud[2], Nadege Loaëc[3], Naïg Gueguen[2], Valérie Desquiret-Dumas[2], Bénédicte Lelievre[4], Aurore Inisan[2], Cristina Panozzo[5], Genevève Dujardin[6], Marc Blondel[3], Agnes Rötig[7], Véronique Paquis-Flucklinger[8], Stéphane Azoulay[9], Nathalie Bonnefoy[6], Carole H. Sellem[6], Agnès Delahodde[6,‡], Vincent Procaccio[2,*], Déborah Tribouillard-Tanvier[1,*,†]

[1]Univ. Bordeaux, CNRS, IBGC, UMR 5095, Bordeaux F-33000, France
[2]Univ Angers, CHU Angers, INSERM1083, CNRS6015, MITOVASC, MITOLAB, SFR ICAT, Angers F-49000, France
[3]Univ Brest; Inserm UMR1078; Etablissement Français du Sang (EFS) Bretagne; CHRU Brest, Hôpital Morvan, Laboratoire de Génétique Moléculaire, Brest F-29200, France
[4]Department of Pharmacology and Toxicology, University Hospital, University of Angers, IRF (Infections Respiratoires Fongiques) Angers 49933, France
[5]Institut de Biologie Physico-Chimique, UMR8226, CNRS, Sorbonne Université, Paris F-75005, France
[6]Université Paris Saclay, CEA, CNRS, I2BC, Gif-sur-Yvette F-91190, France
[7]Université Paris Cité, Imagine Institute, Genetics of Mitochondrial Diseases, INSERM UMR 1163, Paris, France
[8]Université Côte d'Azur, Inserm U1081, CNRS UMR7284, IRCAN, CHU de Nice, Nice F-06107, France
[9]Université Côte d'Azur, CNRS UMR 7272, ICN, Nice F-06108, France

[*]Corresponding authors. Déborah Tribouillard-Tanvier, Univ. Bordeaux, CNRS, IBGC, UMR 5095, Bordeaux F-33000, France.
E-mail: deborah.tribouillard-tanvier@ibgc.cnrs.fr; Vincent Procaccio, Univ Angers, CHU Angers, Inserm, CNRS, MITOVASC, MITOLAB, SFR ICAT, Angers F-49000, France. Email: vincent.procaccio@univ-angers.fr
[†]Research associate from INSERM.
[‡]Passed away.
[§]Co-first authors in alphabetic order.

Abstract

The copper ionophore disulfiram (DSF) is commonly used to treat chronic alcoholism and has potential anti-cancer activity. Using a yeast-based screening assay of FDA-approved compounds, DSF was herein identified for its ability to improve oxidative phosphorylation-dependent growth of various yeast models of mitochondrial diseases caused by a wide range of defects in ATP synthase, complexes III and IV, cardiolipin remodeling, maintenance and translation of the mitochondrial genome. This compound also showed beneficial effects in cells derived from patients suffering from Barth or MELAS syndromes, two mitochondrial diseases associated respectively with a lack in cardiolipin remodeling and protein synthesis inside the organelle. We provide evidence that the rescuing activity of DSF results from its ability to transport copper ions across biological membranes. Indeed, other copper ionophores (pyrithione and elesclomol) and supplementation of the growth media with copper ions had also beneficial effects in yeast and human cells with dysfunctional mitochondria. Our data suggest that the copper-dependent rescuing activity in these cells results from a better capacity to assemble cytochrome c oxidase. Altogether, our findings hold promise for the development of new therapeutic strategies for mitochondrial disorders.

Graphical Abstract

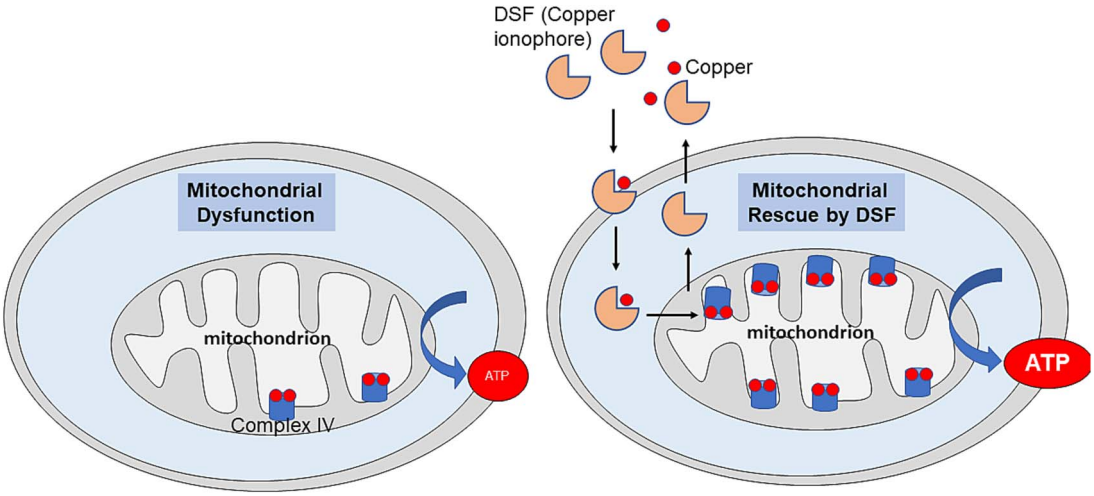

Keywords: Mitochondrial diseases; oxidative phosphorylation; drug repositioning; disulfiram; copper

Introduction

A growing number of human diseases are found to result from inherited or *de novo* mutations in nuclear and mitochondrial genes required for the production of the energy-rich adenosine triphosphate (ATP) molecule, through the process of oxidative phosphorylation (OXPHOS). These diseases, referred to as mitochondrial diseases (MD), affect at least 1 in 5000 live human births [1], and can become symptomatic during infancy or adulthood, in a multisystemic or highly tissue-specific manner. Typical clinical traits include encephalopathies, cardiomyopathies, myopathies, visual/hearing defects, diabetes, liver and renal dysfunctions [2–4].

Despite considerable progress in defining the pathogenesis of MD, most are still awaiting effective therapies. Metabolic or pharmacological treatments including vitamins or cofactors involved in energy metabolism, enzyme activators and anti-oxidants have been tested but conclusive therapeutic benefit was not observed [5, 6]. One approach to develop new drugs against MD is the repositioning of drugs already used in human health with known pharmacokinetics, pharmacodynamics and toxicity data, thus reducing the time and costs of drug development [7]. We have proposed such a strategy using the yeast *Saccharomyces cerevisiae* [8]. This unicellular fungus can survive mutations that inactivate OXPHOS owing to its good fermentative capacity, and is amenable to manipulations of both its nuclear and mitochondrial genomes [9]. Moreover, it contains orthologs of many of the genes involved in mitochondrial structure and function in humans. These features enable the modeling of human MD in a simple eukaryote. When mitochondrial function is compromised, which is often the case with these models, growth is slow from non-fermentable carbon sources (glycerol, lactate, and ethanol) that require OXPHOS to be fully metabolized. Drugs that improve OXPHOS-dependent growth can then be readily identified using a simple solid plate assay that allows the rapid testing of thousands of FDA-approved compounds over a wide range of concentrations in a single experiment [10–12]. Using this approach, we herein report the selection of disulfiram (DSF) for its capacity to improve mitochondrial function in various yeast and human cellular models of MD with defects in ATP synthase, complexes III and IV, cardiolipin remodeling, maintenance and translation of the mitochondrial genome. This drug is commonly used since over 70 years as a first-line treatment for chronic alcoholism and it also holds promise as an anticancer agent [13–15]. We provide evidence that the beneficial effects of DSF in dysfunctional mitochondria are linked to its copper ionophore activity.

Results

Overview of the yeast models of mitochondrial disease used in this study

The yeast models of human MD used in this study result from defects in various mitochondrial processes and components: (i) mitochondrial translation, due to a single A-to-G change at position 29 of the mitochondrially encoded leucine transfer RNA (this model is designated by $tRNA^{Leu}$ in this study); (ii) the assembly of the catalytic F_1 component of ATP synthase, due to the loss of a protein (Fmc1) involved in this process (*fmc1* model); (iii) and (iv) the biogenesis of complex IV, due to a mutation in mtDNA that compromises the synthesis of its Cox2 subunit (*cox2* model) or a nuclear missense mutation (G137R) in the Shy1 protein (*shy1* model); (v) the assembly of complex III, due to a missense mutation (F401I) in the Bcs1 protein that compromises the incorporation of the Rieske iron sulfur protein into this complex (*bcs1* model); (vi) mtDNA synthesis, due to a missense mutation (G651) in mitochondrial DNA polymerase (*mip1* model); (vii) the remodeling of cardiolipin, due to the loss of an acyltransferase (Taz1) involved in this process (*taz1* model); and (viii) the stability of mtDNA, due to the loss of a mitochondrial protein (Sym1) of yet-unknown function (*sym1 model*). The corresponding diseases and origins of the yeast mutants are listed in Table 1 (see also Materials and Methods).

Disulfiram improves respiration-dependent growth of various yeast models of mitochondrial diseases

Chemical libraries mostly composed of FDA-approved compounds were used to identify molecules showing beneficial effects in

Table 1. Genotypes and origins of yeast strains.

Strain	Nuclear genotype	mtDNA	Plasmid	Source
$tRNA^{Leu}$	MCC123: *MATα, his3–11, ade2–1, leu2–3112, ura3–1, trp1-D2, can1–100, syn*$^{-}$	ρ^{+} $tRNA^{Leu}$A30(29)G	ø	[17]
mip1	DWM-5A: *Mat a ade2–1 leu2–3, 112 ura3–1 trp1–1 his3–11, 15 can1–100 mip1::kanMX6*	ρ^{+}	pFL39-mip1^{G651S}	[19]
bcs1	W303: *MATa ade2–1 ura3–1 his311, 15 trp1–1 leu2–3112 can1–100 bcs1*^{F401I}	$\rho+$ intron-less	ø	[20]
cox2	D273: *MATa lys2 leu2–3112 ura3–52 his3DHindIII arg8::hisG*	ρ^{+} *cox2–22*	ø	[18]
shy1	W303: *MATa ade2–1 ura3–1 his311, 15 trp1–1 leu2–3112 can1–100 shy1*^{G137R}	$\rho+$ intron-less	ø	This study
taz1	W303: *MATa ade2–1 ura3–1 his311, 15 trp1–1 leu2–3112 can1–100 taz1::TRP1*	$\rho+$	ø	[21]
sym1	W303: *MATa ade2–1 ura3–1 his311, 15 trp1–1 leu2–3112 can1–100 sym1::kanMX6*	$\rho+$	ø	This study
fmc1	MR6: *MATa ade2–1 his3–11,15 trp1–1 leu2–3112 ura3–1 fmc1::HIS3*	$\rho+$ intron-less	ø	[22]

the eight yeast models of MD described above. To this end, cells from these strains grown in rich glucose medium were spread as dense layers at the surface of solid media containing a non-fermentable substrate (glycerol or ethanol) where they proliferate slowly compared to WT cells. The cells were then exposed to paper disks spotted with the molecules to be tested (2 μl of 10 mM in DMSO) and the plates were incubated for several days at 28°C (*shy1*, *bcs1*) or 36°C (*taz1*, *sym1*, *fmc1*, *mip1*, *cox2* and $tRNA^{Leu}$). As a negative control, each plate contained a paper disk spotted with 2 μl of DMSO. In this assay, the positive hits are identified by halos of enhanced growth around the paper disks. Due to their diffusion in the growth medium, the molecules establish a gradient of concentrations around the paper disks [16], which allows identifying molecules that have beneficial effects only at low concentrations while being toxic at higher concentrations.

As is usually the case, a dozen of positive hits with varying levels of rescuing activity were selected for each screening assay (which corresponds to 1%–2% of active compounds). Remarkably, two of them, among which disulfiram, induced a halo of enhanced respiratory growth with each of the eight yeast disease models described above (Fig. 1A), and this effect was dose-dependent (Fig. 1B). In liquid cultures of strains *taz1*, $tRNA^{Leu}$ and *sym1*, DSF was active within a rather large window of concentrations ranging from 10 nM to 3 μM, while toxic effects were observed at higher concentrations (Fig. 1C). A drug active against multiple mitochondrial dysfunctions is especially interesting for the development of large spectrum therapeutic options (see Table 3). Furthermore, DSF is well tolerated in humans, it has a well characterized pharmacodynamic profile, has been widely used for over 70 years as a first-line treatment for chronic alcoholism and it holds promise as an anticancer agent. For all these reasons we decided to investigate further the therapeutic potential of DSF against mitochondrial diseases, as described in the following sections (the other drug showing beneficial effects in a large panel of yeast mitochondrial disease models will be described elsewhere).

Disulfiram stimulates mitochondrial respiration and complex IV biogenesis in yeast models of human diseases

The yeast mutant strains used in this study show a diminished capacity to transfer electrons to oxygen compared to WT yeast. Furthermore, for reasons that will be discussed below, they have a reduced content in complex IV (cytochrome *c* oxidase) ([17–23], Supplemental Fig. 1 and Fig. 2)). When grown in the presence of 1 μM DSF (from glycerol or ethanol), the mutant cells consumed oxygen more rapidly compared to the same cells not exposed to the drug (Fig. 2A). The influence of DSF on the abundance of complex IV was evaluated by measuring the steady state levels of the Cox2 subunit of this complex. When not assembled, this protein is rapidly degraded, thus serving as a good indicator of the content in assembled complex IV. As shown in Fig. 2B and Supplemental Fig. 3, the strains *taz1*, $tRNA^{Leu}$, *sym1* and *cox2* showed increased Cox2 levels when they were grown in presence of DSF relative to untreated cells. Other mitochondrial proteins, in the intermembrane space (cytochrome b_2) or the mitochondrial inner membrane (Atp6), remained mostly unaffected by DSF (Supplemental Fig. 3), indicating that a general stimulation of mitochondrial biogenesis was not responsible for the DSF-mediated increase in Cox2 accumulation. Taken together, these observations revealed that DSF truly improves oxidative phosphorylation in yeast deficient mitochondria.

DSF-mediated rescue of yeast mitochondrial mutants results from improved transport of copper ions into cells

DSF is known to inhibit aldehyde dehydrogenase (ALDH) and this effect is at the basis of treatment against alcoholism [24, 25]. Other compounds known to inhibit this enzyme, tolbutamide (TBM) and chlorpropamide (CHP), at concentrations 6.6-fold higher than DSF, failed to improve respiratory growth of strains $tRNA^{Leu}$ and *cox2* (Fig. 3A). This indicates that modulation of ALDH activity is likely not involved in the rescue of these strains upon exposure to DSF. We therefore considered another well-known property of DSF, which is its ability to transport copper ions across biological membranes [26]. Interestingly, two other copper ionophores, pyrithione and elesclomol, improved the respiratory growth of strains $tRNA^{Leu}$ and *cox2* (Fig. 3B) and the sole addition of copper ions to the growth media had beneficial effects too (Fig. 3C). Taken together these observations indicate that the beneficial effects of DSF in yeast deficient mitochondria result from the copper ionophore activity of this drug. Unlike elesclomol, DSF would be unable to reach the mitochondrion [27, 28]. However, we found that upon exposure to DSF a strain lacking the main copper transporter (Ctr1) located in the plasma membrane fully recovered the

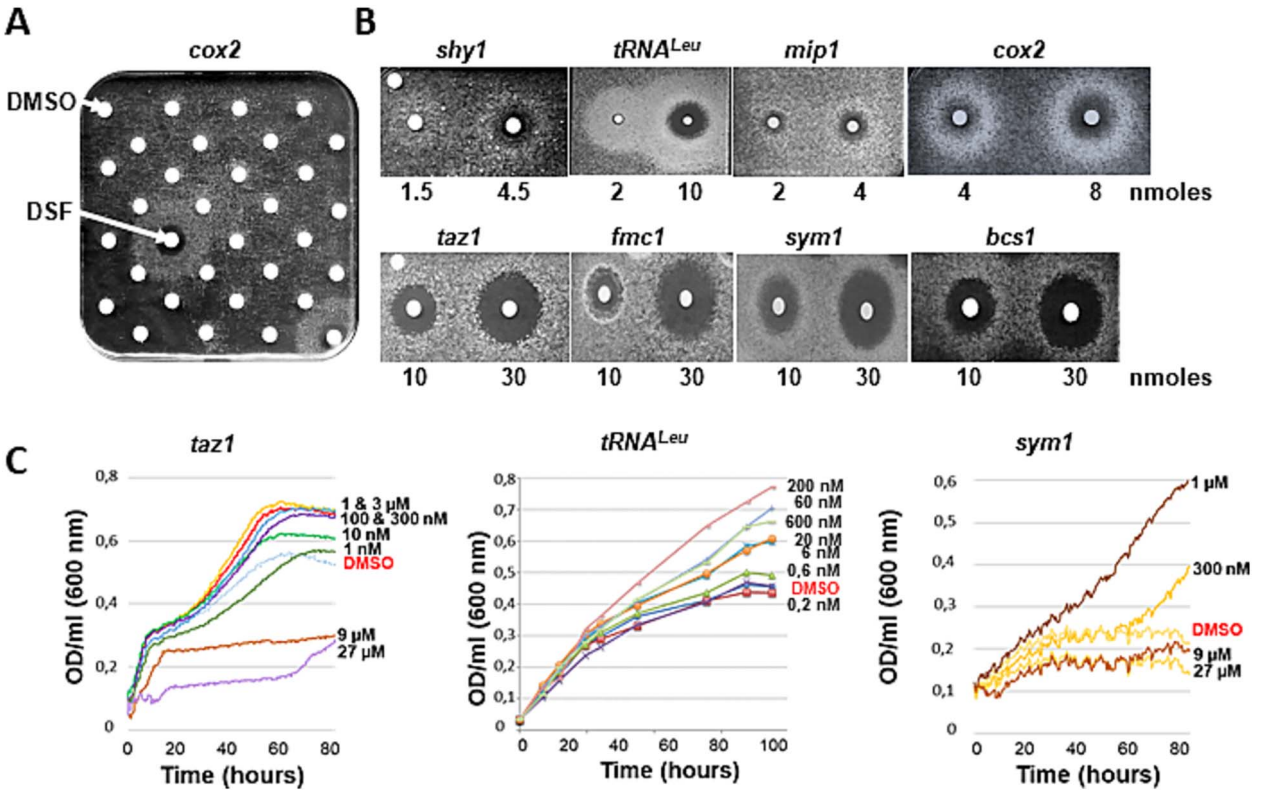

Figure 1. Disulfiram (DSF) improves respiratory growth of different yeast models of mitochondrial diseases. (A) Identification of DSF in chemical screening. 0.125 OD of the yeast mutant cells freshly grown in glucose were homogeneously spread with sterile glass beads on a solid glycerol medium in a square petri dish (12 cm × 12 cm). The cells were then exposed to 20 nmoles dissolved in 2 μl DMSO of compounds from FDA-approved chemical libraries (Prestwick and TebuBio) spotted on paper disks. On each plate, DMSO is used as a negative control (top left filter). The plates were photographed after 4–5 days of incubation at 28°C or 36°C as appropriate (see Table 2). Positive hits are identified by the appearance of a halo of enhanced growth around the filters onto which they were deposited. On the shown plate, DSF improves the growth of *cox2* mutant cells. *B, C. DSF-mediated rescue is dose-dependent*. On solid medium. (B) The eight yeast models tested in this study were spread as dense layers on solid respiratory medium and then exposed to paper disks spotted with the indicated quantities of DSF for 4–7 days at 28 or 36°C (see Table 2). In liquid medium (C). Respiratory medium (see Table 2) supplemented or not with various concentrations of DSF was inoculated with cells from the yeast *taz1*, $tRNA^{Leu}$ or *sym1* mutants pre-grown in rich glucose medium at 28°C. The cultures were performed at the restrictive temperature specific to each strain (see Table 2) under constant shaking and cell densities (OD_{600nm}) were measured at regular intervals over a period of 4 days. The graphs are representative of four independent experiments. For the sake of simplicity and consistency across the strains, an effective concentration of 1 μM was chosen for all tests and for all strains.

ability to grow from respiratory carbon sources (Fig. 3D). As the failure of this mutant to grow by respiration is due to a virtual absence of complex IV [29], it can be inferred that DSF is able to deliver copper ions into mitochondria from the outside of the cell. Not surprisingly, while copper ion supplementation improved respiration-dependent growth of strains $tRNA^{Leu}$ and *cox2*, it failed to do so (at the same concentration) with *ctr1* mutant due to a block in copper transport across the plasma membrane.

The rescuing activity of DSF is not due to altered cellular/mitochondrial redox states or enhanced ROS production

As DSF vehiculates a redox-active metal, we explored the possibility that changes in the redox status of the cell or mitochondria might be involved in its capacity to improve oxidative phosphorylation in yeast strains with dysfunctional mitochondria. To this end we examined the growth of these mutants in media supplemented with five reducing compounds: ascorbate (As), dithiothreitol (DTT), β-Mercaptoethanol (βME), tris(2-carboxyéthyl)phosphine (TCEP) and N-acetylcysteine (NAC). None of them had a visible effect on the growth of the mutant strain *cox2* (Fig. 4A). As a control of the efficacy of the products, the hypersensitivity of a yeast mutant lacking superoxide dismutase (*sod1*) to H_2O_2 was as expected largely suppressed by the reducing compounds (shown for As in Fig. 4B). These observations indicate that the rescuing activity of DSF in dysfunctional mitochondria did not result from changes in the redox status of the cell or mitochondria.

Another track we then explored concerns the property of DSF in combination with copper ions to promote formation of ROS [30]. If in high amounts these can have strong detrimental cellular consequences, ROS would have in limited quantities beneficial effects on mitochondrial function and biogenesis through a mitochondrion-to-nucleus retrograde response [31, 32]. At the concentrations of DSF (1 μM) with the best effects on the respiratory growth of yeast models of mitochondrial diseases, we detected a significant increase in ROS levels compared to the DMSO control (Fig. 4C). If this effect would have some role, reducing compounds with antioxidant activity should prevent DSF to stimulate oxidative phosphorylation in dysfunctional mitochondria. This was not observed. The beneficial effects of DSF in the *cox2* mutant were indeed largely preserved in the presence of ascorbate (As) or TCEP (Fig. 4D) (these two compounds do not contain thiol groups that have the potential to chelate copper ions like NAC, DTT, and βME, which for this reason were not tested in combination with DSF). Consistently, DSF significantly improved respiratory growth of the yeast mutant lacking superoxide dismutase (Sod1), a copper-containing enzyme that protects the

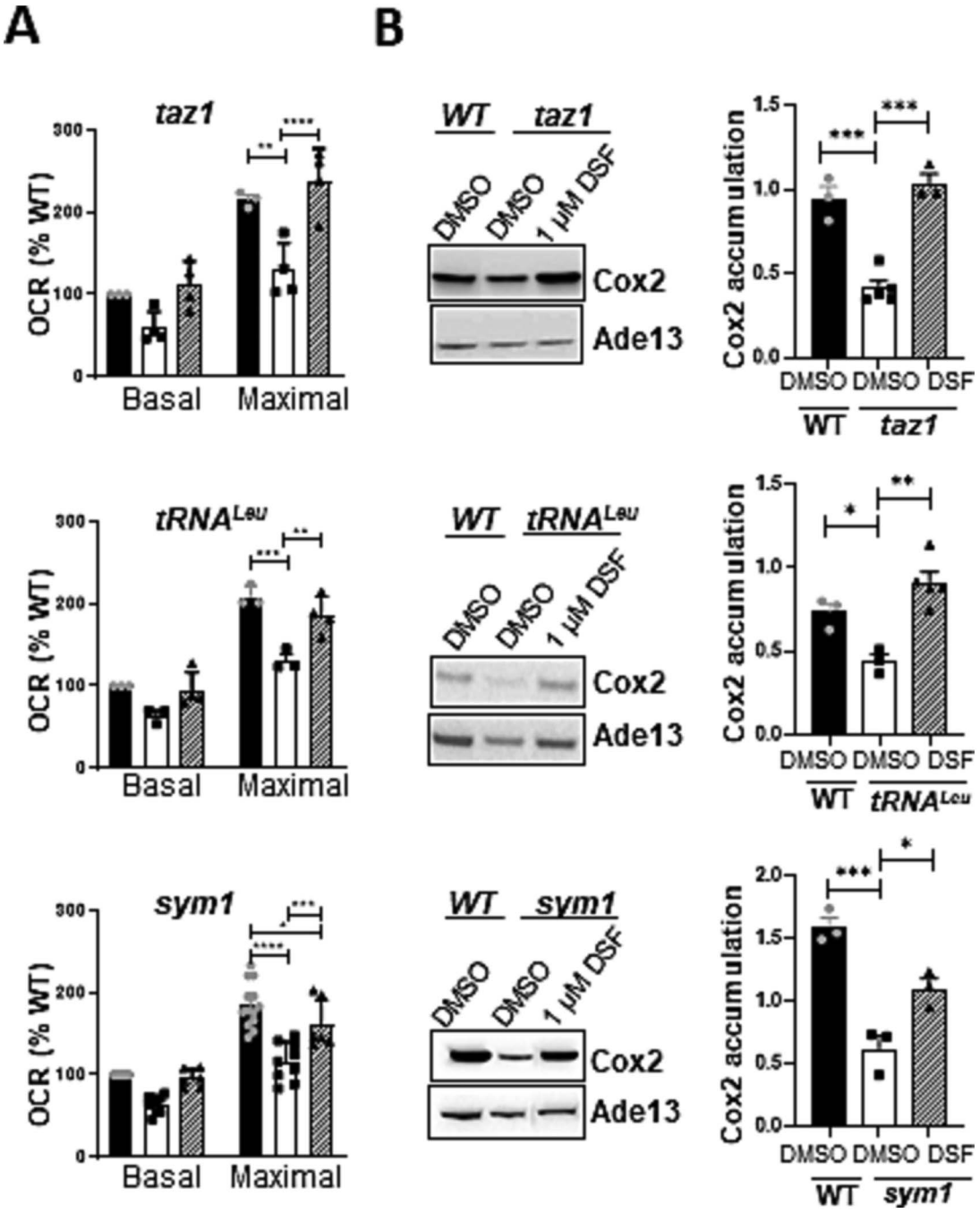

Figure 2. *Influence of DSF on cellular respiration and accumulation of complex IV in yeast mitochondrial deficient mutants.* (A) *Cellular respiration.* 10^7 cells from WT (black bar) and *taz1*, $tRNA^{Leu}$ or *sym1* mutant cells grown for 7–8 generations at restrictive temperature in respiratory medium (see Table 2) in absence (DMSO control, white bar) or presence of 1 μM DSF (hatched bar) were tested for oxygen consumption. Oxygen consumption rates (OCR) were recorded without any substrate addition (basal), and after inhibiting ATP synthase with oligomycin and fully uncoupling mitochondria with CCCP (maximal). Non-mitochondrial respiration observed after inhibiting complex III with antimycin a has been subtracted from the OCR. (B) Steady-state levels of Cox2. Total protein extracts of the indicated yeast mutant strains were resolved by SDS-PAGE, transferred onto a nitrocellulose membrane and probed with antibodies recognizing Cox2 or the non-mitochondrial Ade13 protein used as a loading control. The levels of Cox2 normalized to Ade13 in the different samples are compared to the DMSO controls.

cell against oxidative damage (Fig. 4E). This observation rules out the possibility that a better delivery of copper ions into this enzyme and thus a stronger capacity to scavenge ROS contributes in some way to the rescuing activity of DSF in the *cox2* mutant. In line with this, exposure of this mutant to oxygenated water did not improve its growth from respiratory carbon sources (Fig. 4A).

It is interesting to note that the toxicity of DSF at high concentrations (near the paper disks) was largely reversed upon addition of copper ions. Possibly at these concentrations, there is a competition for copper ions between DSF and those cellular systems (among which complex IV) that use copper ions as a cofactor. Ascorbate also mitigated the toxicity of DSF at high concentrations, which is not very surprising since in these conditions DSF can induce oxidative damage. Consistently, the toxicity of DSF was mostly suppressed upon exposure to both copper ion supplements and ascorbate (Fig. 4F).

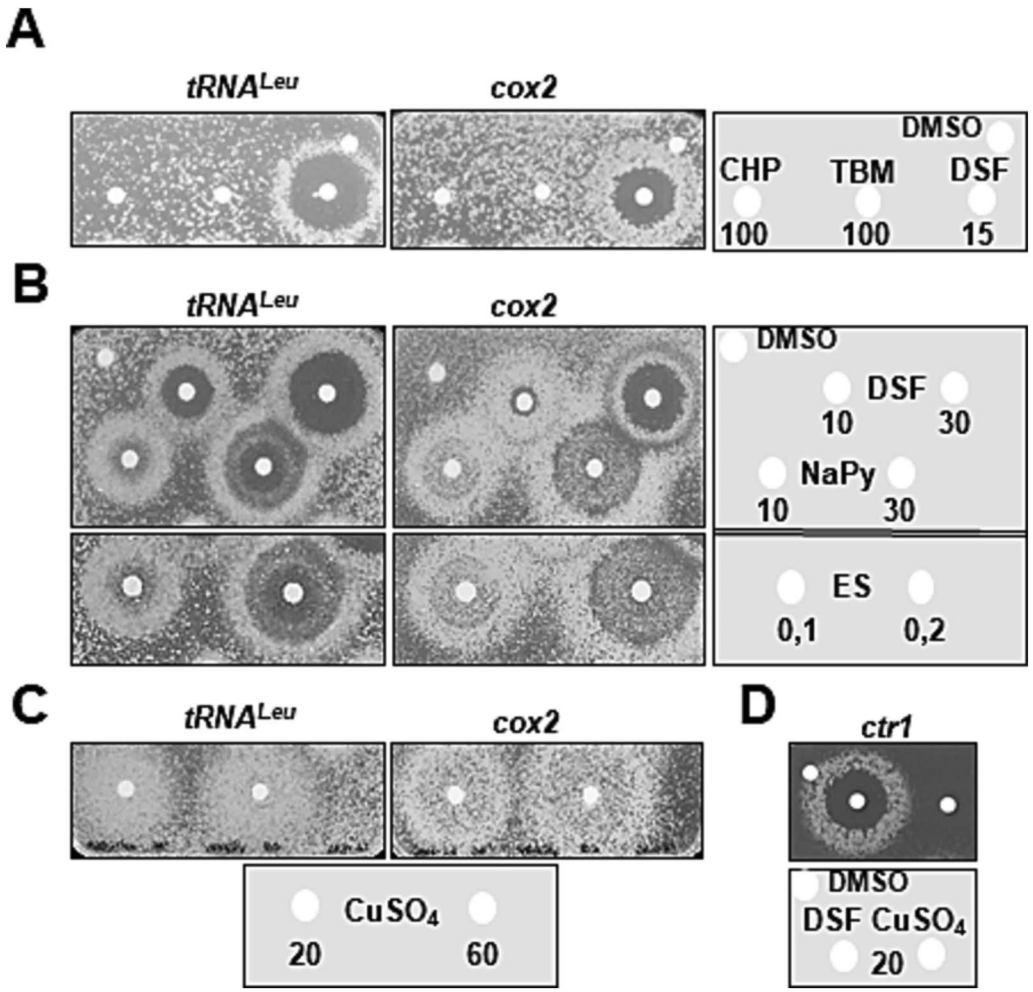

Figure 3. The beneficial effect of DSF in yeast models of mitochondrial diseases is linked to the copper ionophore activity, not its capacity to inhibit ALDH. *A, B, C. Tests with the ALDH inhibitors chlorpropamide (CHP) and tolbutamide (TBM) (A), with the copper ionophores sodium pyrithione (NaPy) and elesclomol (ES) (B), or with supplements of copper ions (C).* Cells from $tRNA^{Leu}$ *and cox2* mutant yeast strains grown in rich liquid glucose medium were spread as dense layers onto rich respiratory glycerol solid medium and then exposed to sterile filters spotted with the indicated amounts in nmoles of the different drugs, as well as DMSO alone as a negative control, as indicated by each scheme. The DMSO control corresponding to the spots shown in panel 3C is the one in panel 3B. The spots in these two panels are indeed from the same plate. The plates were scanned after 5 days of incubation at the appropriate temperature (see Table 2). *(D) DSF restores the growth on glycerol of a mutant yeast strain (ctr1) lacking the major plasma membrane copper transporter Ctr1.* Cells from *ctr1* cells grown in rich liquid glucose medium were spread as a dense layer onto rich glycerol solid medium and exposed to paper disks spotted with 20 nmoles of DSF or 20 nmoles of $CuSO_4$, or with DMSO alone as a negative control, as indicated by the associated schemes. The plates were scanned after 4 days of incubation at 28°C.

Taken together these observations lead us to conclude that the beneficial effects of DSF in yeast dysfunctional mitochondria are mainly due to enhanced complex IV biogenesis and not to altered cellular redox changes or a general ROS-mediated stimulation of mitochondrial biogenesis.

DSF stimulates the respiratory growth of wild type yeast without changes in the cellular content of complex IV

Since copper ions (added alone or vehiculated by DSF) improved respiration in a wide variety of yeast strains with dysfunctional mitochondria, we wondered whether they could also stimulate mitochondrial function in WT yeast. To this end, the mutant strains *cox2* and *taz1* and their parental strains (respectively NB80 and W303–1B) were grown for 2–3 days in rich liquid medium containing a non-fermentable carbon source, with or without 300 μM or 1 mM of $CuSO_4$. As expected from the results described above, the $CuSO_4$ supplements resulted in higher optical densities for both mutant strains (Fig. 5A) and significantly increased the steady state levels of the Cox2 subunit in comparison to the DMSO controls (Fig. 5B). When samples of the cultures were tested on solid glycerol plates lacking copper supplements, the respiratory growth deficient phenotype of the *cox2* and *taz1* strains was readily observed, demonstrating that the beneficial effects of copper ions in the liquid cultures were not due to genetic reversions (Fig. 5C). Both WT strains grew much better also when provided with $CuSO_4$ supplements (Fig. 5A) but their Cox2 cellular contents did not change significantly (Fig. 5B). A possible explanation for these observations is provided below.

DSF and copper ions have beneficial effects in patient's cells with defects in cardiolipin remodeling or mitochondrial translation

As an important step toward translational development of the observations made with yeast, we tested the effects of DSF or copper supplements in MELAS cybrids and cells derived from BTHS patients. These cells carry mutations that compromise respectively the incorporation of leucine residues into mtDNA

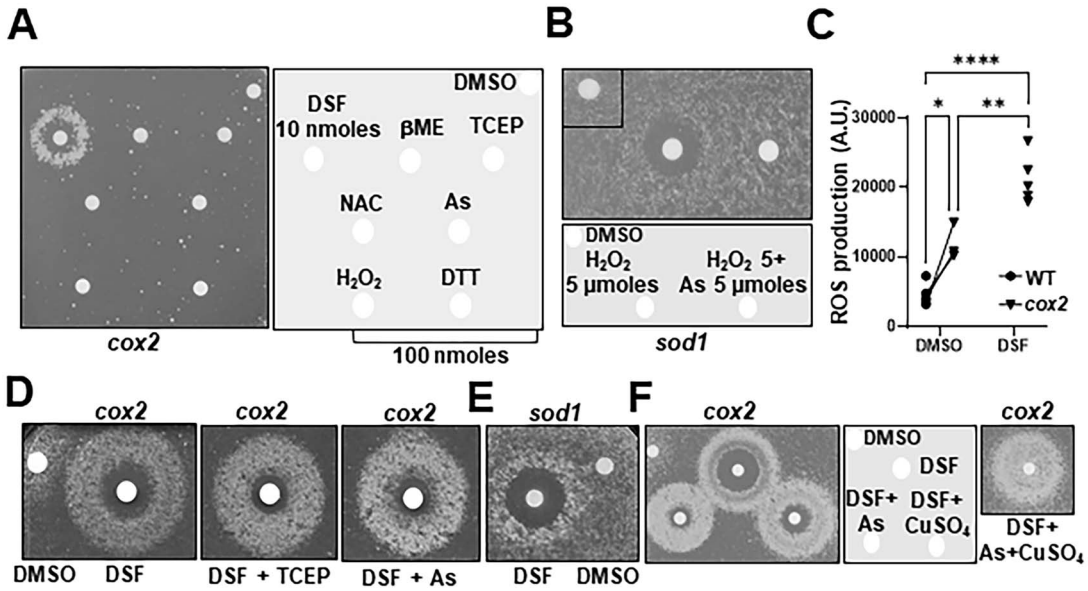

Figure 4. The rescuing activity of DSF is not due to altered cellular redox states or increased ROS production. A, B, D, E, F. Filter disk assays on *sod1* and *cox2* mutants. The *sod1* and *cox2* mutant strains were spread as dense layers on solid YPG respiratory medium and exposed to paper disks spotted with: 10 nmoles of DSF or 100 nmoles of As, DTT, βME, TCEP, NAC, or H_2O_2 (*cox2* mutant, A); H_2O_2 alone (5 μmoles) or in combination with ascorbate (As, 5 μmoles) (*sod1* mutant, B); 20 nmoles of DSF alone or combined with 200 nmoles of TCEP or As (*cox2* mutant, D); 20 nmoles of DSF (*sod1* mutant, E); 30 nmoles of DSF alone or in combination with 1 μmole of As and/or 10 nmoles of $CuSO_4$ (*cox2* mutant, F). DMSO alone is the negative control. Plates were scanned after 4 days incubation at 28°C for *sod1* mutant and 36°C for *cox2* mutant. C. ROS production in the *cox2* mutant. WT (circles) and *cox2* mutant (triangles) cells were grown in respiratory medium with or without 1 μM DSF at 36°C for 96 h. ROS levels were measured by flow cytometry using dihydroethidium as a probe. Statistical significance was assessed.

encoded polypeptides and cardiolipin. We first characterized the influence of DSF on the rate of proliferation of BTHS myoblasts and fibroblasts exposed to various concentrations of DSF during 4–5 days *vs* untreated cells (DMSO controls). Several-fold increases in cell densities were induced by the drug within a rather large window of picomolar-to-micromolar concentrations above which cell proliferation was virtually abolished (Fig. 6A and Fig. 6B). The rate of oxygen consumption related to complex I respiration in MELAS cybrids grown in the presence of copper ions supplements (Fig. 6C) was considerably increased compared to untreated cells. Mitochondria purified from MELAS neuronal cybrids grown in the presence of DSF showed a 2-fold increase in copper content compared to those from mutant cells not exposed to the drug (Fig. 6D). The rate of oxygen consumption related to complex I respiration was significantly increased in MELAS cybrids exposed to 10 nM DSF compared to vehicle (Fig. 6E). As shown previously [33] complex I respiratory rate was 50% lower in MELAS neuronal cybrids compared to SH-SY5Y WT cells. Similar to the wild type yeast, DSF had beneficial effects on cellular proliferation of control human cells (Fig. 6F). We finally probed the influence of DSF on the levels of the COX2 subunit of complex IV in the MELAS cybrids. As expected, there was a substantial decrease in the content of COX2 in the mutant versus control cells. As with the yeast models of mitochondrial diseases, the COX2 protein accumulated more in the MELAS cybrids when they were exposed to DSF whereas the drug had no significant influence on COX2 in control cells (Fig. 6G). If the SOD1 protein was present in higher amounts in the mutant versus wild type cells (which is a common property of mitochondrial deficient cells [34]), it did not show further increase upon exposure of the cells to DSF (Fig. 6G). Taken together, these observations reveal that the copper ionophore activity of DSF has beneficial effects on mitochondrial function in both yeast and human cellular models of MD.

Discussion

DSF has been used for decades in the treatment of alcoholism as a medicine called antabuse, due to its ability to inactivate ALDH [24, 25]. When ALDH activity is compromised, the uptake of alcohol leads to the accumulation of acetaldehyde, triggering several unpleasant effects (dizziness, flushing or headaches). DSF is also a promising drug for the treatment of some types of cancers [15], due to its ability to promote copper-dependent formation of Reactive Oxygen Species (ROS) to which some cancer cells are more sensitive than normal cells. The present study extends the therapeutic potential of DSF to mitochondrial diseases (MD). Indeed, several yeast mutant strains with various mitochondrial dysfunctions at the origin of metabolic disorders (including defects in the assembly/activity of complexes III, IV and V, cardiolipin remodeling, mtDNA maintenance, replication and translation) were found to recover a better capacity to grow from non-fermentable substrates and to transfer electrons to oxygen when exposed to DSF. Other copper ionophores (elesclomol and pyrithione) had similar effects, as well as the sole addition of copper ions to the growth medium. The beneficial effects of DSF in yeast mitochondrial mutants thus clearly result from the ability of this drug to transport copper ions into cells. Importantly, DSF-mediated rescue of yeast and human cellular models of MD occurred at concentrations of DSF much lower than those impairing the viability of human and yeast cells due to extensive oxidative damage (<1 μM *vs* > 50 μM) [26, 35–37]. Thus, while DSF-mediated rescue of dysfunctional mitochondria and the killing of human cancer cells are both copper-dependent, the underlying mechanisms must differ and are concentration-dependent.

A main function of copper ions in cells is the transfer of electrons within complex IV, from cytochrome *c* to oxygen. Incorporation of copper ions into this complex is a sophisticated process that involves several accessory proteins, some of which were

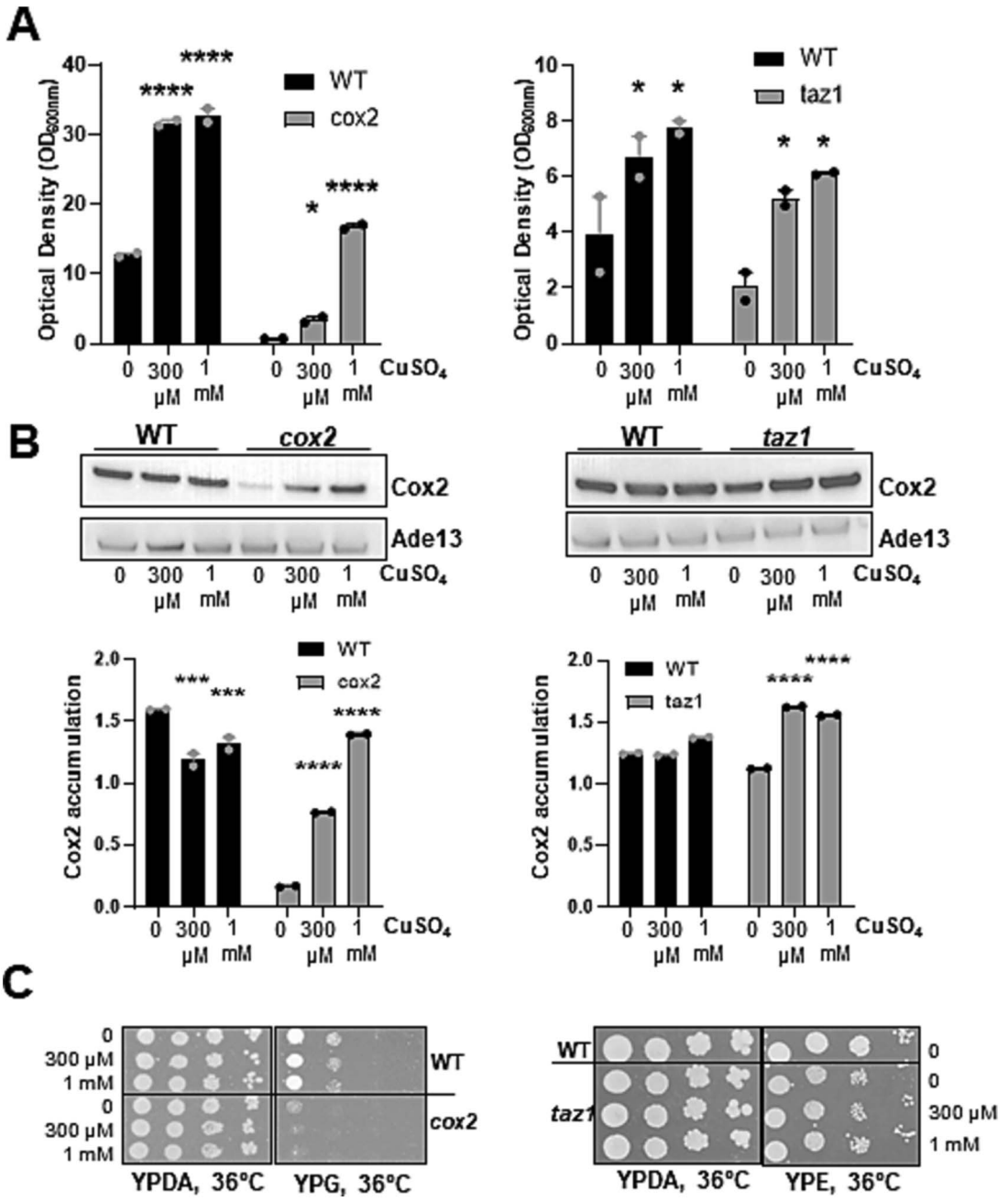

Figure 5. Influence of copper ions supplementation on respiration-dependent growth and cellular content of complex IV in wild type yeast. (*A*) *Respiratory growth*. Glucose grown cells from the *cox2* mutant strain and its parental strain NB80 (left panel), and from *taz1* mutant and its parental strain W303–1B (right panel) were inoculated in respiratory medium supplemented with the indicated concentrations of copper ions ($CuS0_4$) or DMSO alone (negative control, noted as 0) and incubated at the restrictive temperature of 36°C. Cell densities were recorded after 72 h (*cox2* left panel) or 48 h (*taz1* right panel). (*B*) *Steady-state accumulation of Cox2*. Total protein samples (50 μg) prepared from the cultures tested in *panel a* were run in SDS gels, transferred onto a nitrocellulose membrane and probed with antibodies against Cox2 and Ade13 (upper panel). The levels of Cox2 normalized to Ade13 in the different samples are compared to the DMSO controls (lower panel). (*C*) *Tests for the presence of revertants in the cultures of cox2 and taz1 mutant strains*. Samples from cultures shown in panel a were serially diluted and spotted on rich glucose and glycerol media. The plates were scanned after 5 days of incubation at 36°C.

found to be the target of pathogenic mutations [38, 39]. Yeast and zebrafish models of such mutations in the cytochrome *c* oxidase assembly factor 6 *(Coa6)* were found to be efficiently rescued by elesclomol or copper ion supplementation [40]. Based on direct evidence that elesclomol drives accumulation of extracellular copper ions into mitochondria [41], it was concluded that this molecule can bypass proteins specifically involved in the delivery of copper into complex IV.

However, somewhat remarkably, our study reveals that copper transporters or supplementation also improve mitochondrial function in yeast strains with no primary defect in the pathway that enables incorporation of copper ions into complex IV. Nevertheless, a better capacity to assemble the complex IV is possibly involved also in the copper-dependent rescue of these strains. Previous studies have indeed shown that this complex is the most regulated component of the OXPHOS system, which would

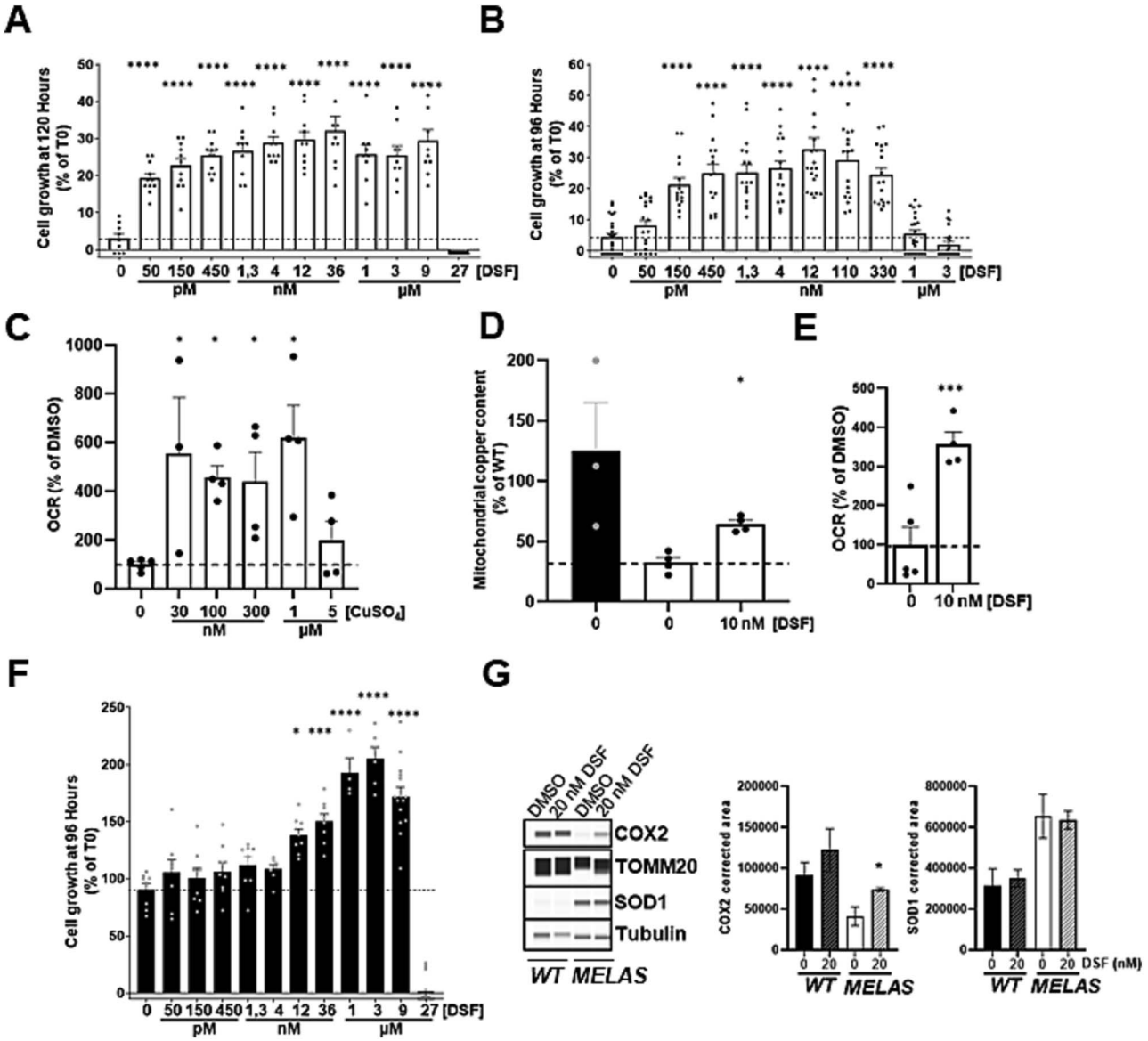

Figure 6. DSF and copper ion supplementation have beneficial effects in MELAS cybrids and cells derived from BTHS patients (*A and B*). *Proliferation of BTHS patient cells in presence/absence of DSF on (A) myoblasts after 120 h in HG medium and on (B) fibroblasts after 96 h in LG* medium. 1200 cells per well were plated in the presence of the indicated concentrations of DSF or DMSO as vehicle (noted as 0). The reported growth values in A and B are means calculated from 4 independent experiments, expressed relative to the number of cells at T0. Statistical significance of growth differences versus the DMSO control was estimated. (C) Influence of copper ion supplementation from 30 nM to 5 μM $CuSO_4$ on the rate of oxygen consumption of complex I in MELAS cybrids. Complex I linked respiration was measured from 3.10^6 cells grown for 48 h in LG medium supplemented with either DMSO (noted as 0) or the indicated concentrations of copper after permeabilization with digitonin. The significance of variations among samples vs DMSO was estimated. (D) Influence of DSF on mitochondrial copper content in MELAS cybrids. Copper contents in mitochondria from MELAS cybrids (white bars) grown in LG medium for 48 h supplemented with either DMSO (noted as 0) or 10 nM DSF and from WT cells (black bars) supplemented with DMSO alone were measured using inductively coupled plasma-mass spectrometry (ICP- MS) (7800, Agilent technologies, Santa Clara, USA). The reported data are expressed in % relative to the WT. the significance of variations among samples vs DMSO was estimated. E. Influence of 10 nM DSF after 48 h exposure on the rate of oxygen consumption of complex I in MELAS cybrids compared to DMSO as vehicle. F. Influence of DSF on the growth of control fibroblasts. The cells (1200 per well at T0) from a healthy individual were grown for 96 h in LG medium in the presence of the indicated concentrations of DSF or DMSO as vehicle (noted as 0). The reported growth values are expressed relative to the number of cells at T0. Statistical significance of growth differences versus the DMSO control was estimated. G. Steady-state levels of Cox2 and SOD1. Total protein extracts of WT or MELAS cybrids were resolved by SDS-PAGE, transferred onto a nitrocellulose membrane and probed with antibodies recognizing COX2, SOD1, TOMM20 and the non-mitochondrial tubulin protein used as a loading control. The levels of Cox2 and SOD1 normalized to tubulin in the different samples are compared to the DMSO controls (noted as 0).

enable the cell to balance its needs in ATP to electron transfer to oxygen [42, 43]. The best documented case was provided with studies of yeast ATP synthase defective mutants. For instance, in a yeast strain lacking the mitochondrial *ATP6* gene that encodes an essential subunit of the proton-translocation domain of ATP synthase, there is a 90% drop in the level of complex IV [44]. The underlying mechanism would involve a hyperpolarization of the mitochondrial membrane and subsequent block in the incorporation of copper into this complex [45]. In favor to this hypothesis, a partial uncoupling of the mitochondrial membrane with CCCP was shown to efficiently restore the assembly of complex IV in ATP synthase defective mutants [43]. As a result, electrons can

be moved faster to oxygen, and this enhances the production of ATP in mitochondria through substrate-level phosphorylation of ADP coupled to TCA-mediated conversion of alpha-ketoglutarate into succinate. Possibly, artificially increasing the concentration of copper ions into cells may stimulate the biogenesis of complex IV when mitochondrial function is compromised. A not-mutually exclusive possibility is that the standard rich media used for growing yeast by respiration are too poor in copper ions and this limits the rate of complex IV biogenesis. This would in fact not be very surprising. Indeed, the main source of copper ions in these media is an extract of yeast cells grown by fermentation (the 'Yeast Extract') and these have a low content in copper due to the large repression in these conditions of complex IV biogenesis (most of the copper present in respiring yeast is by far located within this complex). In support to this hypothesis, copper supplementation was found to stimulate also respiration-dependent growth of WT yeast even though the content in complex IV was not increased. A logical explanation is that this complex assembles faster when more copper is available, and this enable growing cells to reach more rapidly the levels in complex IV that precede a new cellular division.

Support to this hypothesis can be found in a previous study aiming to discover mechanisms able to rescue complex IV defects in human and yeast cells carrying mutations in a conserved protein (called SURF1 in human, Shy1 in yeast), which is involved at early step in the assembly of this complex. This protein would be required for insertion of heme A at the a_3 center or stabilization of the a_3-CuB binuclear center in the Cox1 subunit of complex IV [46]. Although SURF1/Shy1 would not be directly required for insertion of copper ions into complex IV, copper ions supplementation to the growth media was able to substantially improve respiration-dependent proliferation of yeast *shy1* mutants. As suggested, increasing the concentration of copper ions in cells may enhance formation of the two-copper containing redox centers linked to the Cox1 and Cox2 subunits of complex IV. As a result, more stabilized assembly modules with Cox1 and Cox2 subunits in interaction with their partner subunits accumulate, which ultimately leads to higher levels of fully processed complex IV.

Interestingly, mitochondrial function in human cells also benefited from a better supply in copper as evidenced by (i) the much faster proliferation of cells derived from BTHS patients when exposed to DSF, (ii) a three-fold stimulation of oxygen consumption and significant increase in mitochondrial copper content and COX2 in MELAS cybrids grown in the presence of DSF or media enriched with copper ions, and (iii) the ability of control cells to grow more rapidly in the presence of DSF. The extension to human cells of the beneficial effects of copper supplementation observed in yeast is consistent with our hypothesis that copper-mediated mitochondrial function stimulation involves a highly conserved process, namely the biogenesis of the catalytic core of complex IV.

Copper homeostasis is a highly regulated cellular process [47], in particular at the level of copper transport across membranes and distribution within cellular systems, and protection against oxidative damage to prevent copper ions to promote the production of reactive oxygen species (by the Fenton reaction) especially in the reducing environment of the cell (mono-cationic copper has a high propensity to generate oxygen radicals). In the presence of copper ionophores, beyond a certain threshold, uncontrolled entry of copper ions into cells certainly compromises copper homeostasis, which is exploited to control proliferation of cancer cells that are particularly sensitive to oxidative damage [48]. Such deleterious effects do not occur at the much lower concentrations of copper ionophores we found to improve mitochondrial function in healthy and mitochondria-deficient yeast and human cells. However, a slight increase in ROS production nevertheless occurs (Fig. 4C), which is likely due to the incapacity of metallothioneins to fully prevent DFS-mediated accumulation of free copper ions in cells. It has been argued that a modest increase in ROS production mediated by pro-oxidant compounds can stimulate mitochondrial biogenesis in yeast cells, which would reflect the existence of ROS-mediated retrograde signaling that aims at modulating expression of nuclear genes with a mitochondrial function in response to the energy-transduction activity of the organelle [31, 32]. Our tests using reducing compounds with a well-established antioxidant activity, alone or in combination with DSF, do not support this possibility. In line with this, DSF improved respiration-dependent growth of yeast mutant lacking superoxide dismutase, which rules out the possibility that the rescuing activity of DSF involves a better delivery of copper ions to this enzyme.

The findings reported in this study lay the groundwork for developing nutritional or metabolic interventions for attenuating the deleterious consequences of multiple mitochondrial dysfunctions at the origin of human diseases.

Materials and methods

Yeast models of mitochondrial diseases

The yeast models of MD used in this study are listed in Table 1. *tRNA^{Leu}* is a yeast model carrying the Mitochondrial Encephalomyopathy—Lactic Acidosis—Stroke like episode (*MELAS*) syndrome mutation m.3260A > G in the mitochondrial tRNA$^{Leu\ (UUR)}$ gene (A30G in patients, A29G in yeast) [17]. *mip1* is a yeast model of Alpers syndrome in which the nuclear *MIP1* gene encoding mitochondrial DNA (mtDNA) polymerase has been deleted (*mip1*::KAN^R) and replaced by a plasmid born version carrying the *mip1^{G651S}* allele equivalent to the human G848S POLG mutation [19]. *bcs1* is a yeast model of GRACILE syndrome where the nuclear *BCS1* gene is mutated to encode the F401I variant, equivalent to the human F368I BCS1L mutation [20]. *shy1 is a* yeast model of Leigh syndrome where the nuclear *SHY1* gene encoding a protein involved in the assembly of complex IV encodes the Shy1-G137R variant equivalent to the human SURF1-G124R mutation (see below for the construction of *shy1* strain). *cox2* is another yeast model of diseases resulting from defects in the assembly of complex IV in which the mtDNA mutation *cox2–22* severely compromises the synthesis and accumulation of the Cox2 subunit of this complex [18]. *taz1* is a yeast model of Barth syndrome where the nuclear gene (*TAZ1*) encoding for an acyltransferase involved in the remodeling of cardiolipin has been deleted [21]. *sym1* is a yeast model of the Navajo hepato-cerebral syndrome in which the yeast homolog of a human protein (MPV17) of unknown molecular function that is required for mtDNA maintenance has been deleted (see below for the construction of *sym1* strain). *fmc1* is a yeast model of cardiomyopathies and neuropathies where a nucleus-encoded protein (Fmc1) involved in the assembly of the F_1 component of ATP synthase has been deleted [22, 23].

Construction of shy1 and sym1 yeast models of mitochondrial diseases

shy1: the *SHY1* gene was deleted in the wild-type (WT) strain CW252 (a W303–1B derivative that contains intron-less mtDNA, see Table 1, [49]) by replacing its open reading frame (ORF) with the *URA3* coding sequence. The nucleotide substitution specifying the G137R variant was introduced into the *SHY1* gene cloned on a plasmid using the Stratagene QuikChange Kit, before integration by homologous DNA recombination at the *shy1::URA3* locus, simultaneously generating uracil auxotrophs. These were selected in the presence of 5-Fluoroorotic acid, that killed uracil

Table 2. Mutant-specific growth conditions used to visualize DSF effect.

Strain	solid medium	Liquid medium	Incubation temperature
$tRNA^{Leu}$	YPG	YPG	36°C
mip1	YPE	YPE	36°C
bcs1	YPG	YPG	28°C
cox2	YPG	YPG + 0,1% galactose	36°C
shy1	YPG	YPG + 0,1% galactose	28°C
taz1	YPE	YPE+0,2% galactose	36°C
sym1	YPE	YPE+0,2% galactose	36°C
fmc1	YPG	YPG + 0,2% galactose	36°C

Depending on the strain, YPG or YPE was preferentially used as the respiratory phenotype was clearer, enabling a more accurate assessment of the drug candidates' beneficial effects. In liquid culture, the phenotype was more severe than in solid medium, and the addition of a small amount of galactose allowed initial cell growth, facilitating a better evaluation of the drug candidates' effects.

Table 3. Effect of DSF on yeast models of various human mitochondrial diseases.

Yeast gene	Human ortholog	Function	Human disease	Respiratory growth on solid medium	Optimal concentration for cell proliferation	Cell Respiration (fold increase relative to mutant)
$tRNA^{Leu(UUR)}$	*MT-TL*	Mitochondrial translation	MELAS	+++	150–200 nM	1,4 $p = 0{,}0002$
MIP1	*POLG*	mtDNA replication	Alpers-Huttenlocher disease/M-NGIE/PEO	+	nd	nd
BCS1	*BCS1L*	CIII assembly	GRACILE/Bjornstad Syndrome	++	nd	nd
COX2	*MT-COX2*	CIV	MELAS, Cytochrome C Oxidase deficiency	+++	300 nM	nd
SHY1	*SURF1*	CIV assembly	Leigh syndrome	+	300 nM	1,15 $p = 0{,}06$
TAZ1	*TAZ*	Cardiolipin remodeling	Barth syndrome	++	1 μM	1,85 $p < 0{,}0001$
SYM1	*MPV17*	mtDNA maintenance	Hepatocerebral syndrome	++	1 μM	1,42 $p = 0{,}0019$
FMC1	*FMC1*	ATP synthase assembly	NARP	++	1 μM	nd

The signs (+, ++, and +++) represent a semi-quantitative assessment of the drug candidate's effect on the different strains based on the halo of growth around the filter where DSF was spotted (Fig. 1). The effect of +++ is greater than ++, which is greater than +.

prototrophs *shy1::URA3* cells that had failed integrating the G137R mutated version [50], and verified by PCR analysis and DNA sequencing. *sym1*: this yeast model was constructed in strain W303–1A (*MATa ade2–1 ura3–1 his311, 15 trp1–1 leu2–3112 can1–100*, see Table 1) by replacing the open reading frame of *SYM1* by that the *kanMX6* marker gene, using a previously described procedure (Longtine et al., 1998). The chromosomal integration of the *sym1::kanMX6* allele was PCR-verified.

Yeast growth media

YPDA is a rich glucose medium used for growing yeast by fermentation: 1% (w/v) yeast extract, 2% (w/v) bacto peptone, 40 mg/l adenine and 2% (v/v) glucose. YPG and YPE are respectively rich glycerol and ethanol media used for growing yeast by respiration: 1% (w/v) yeast extract, 2% (w/v) bacto peptone, 40 mg/l adenine and 2% (v/v) ethanol (YPE) or glycerol (YPG). Solid media contained 2% (w/v) agar. The media and temperatures for growing the different yeast MD models are indicated in Table 2.

Yeast-based drug screening assay

0.125 OD_{600nm} of exponentially growing cells were homogeneously spread with sterile glass beads on a square Petri dish (12 cm × 12 cm) containing solid glycerol or ethanol media. Sterile filters were deposited on the plate and spotted with drugs from Prestwick and Tebu-Bio chemical libraries (most are FDA-approved), dissolved in 2 μl of dimethyl sulfoxide (DMSO) at a typical concentration of 10 mM. Growth improvement was assessed after several days of incubation at the appropriate temperature (see Table 2).

Commercial origins of the drugs and chemicals used in individual tests

Disulfiram (DSF): Sigma PHR1690; tolbutamide (TBM): Sigma 46 968; chlorpropamide (CHP): Sigma PHR1284; sodium pyrithione (NaPy): Sigma H3261; elesclomol (ES): Sigma SML2651; copper sulfate: Merck 3 632 031.

Automatic monitoring of yeast growth

The Bioscreen C microcultivation instrument was used to monitor the growth of yeast strains in 100 μl of respiratory media (see Table 2) supplemented or not with the drugs at the appropriate temperatures (see Table 2) and under continuous shaking. Cell densities (OD_{600nm}) were automatically recorded every 20 minutes over a period of 100 h.

Yeast oxygen consumption

Oxygen consumption of 10^7 cells in the growth medium was measured using an OROBOROS oxygraph system under two different conditions: no addition; addition of 4 μg/ml of oligomycin (Sigma, O4876) to assess the rate of respiration driven by the passive permeability to protons of the mitochondrial membrane; further addition of 1,5 μM carbonylcyanure m-chlorophénylhydrazone (CCCP) to fully uncouple the mitochondrial membrane (maximal respiration). Non-mitochondrial respiration was measured in the presence of 2 μg/ml of antimycin A (Sigma A8674) to calculate mitochondrial-dependent oxygen consumption rates.

Yeast cytochromes

Low temperature cytochrome spectra were recorded with a Cary 400 (Varian, San Fernando, CA) spectrophotometer from whole yeast cells supplemented with the reducing agent sodium hydrosulfite just before freezing in liquid nitrogen. For each spectrum, 10^{10} cells ($OD_{600} = 6$) grown in liquid galactose medium were collected. Absorption spectra show four main peaks corresponding to the cytochromes *c*, cytochromes *c1* and *b* of complex III and cytochrome $a + a3$ of complex IV at 546, 552, 558 and 602 nm respectively. The heights of the different cytochrome peaks were measured to perform semi-quantitative analysis.

ROS analysis

Yeast cells at 0.4 OD units were taken from liquid cultures, pelleted in a microcentrifuge, resuspended in 1 ml of phosphate-buffered saline (PBS) containing 50 μM dihydroethidium (DHE; Molecular Probes) and incubated at room temperature for 5 minutes. Flow cytometry was carried out on a Becton-Dickinson Accuri C6 model flow cytometer. The DHE fluorescence indicated was the direct output of the FL2A (red fluorescence) channel without compensation. A total of 100 000 cells were analyzed for each curve.

SDS-PAGE and western blotting of total yeast proteins

10 OD_{600nm} of cells were collected and resuspended in 500 μl of 0.2 M NaOH. After 10 minutes incubation on ice, the samples were mixed with 50 μl of 50% trichloroacetic acid, incubated for 10 minutes on ice, and centrifuged at 21950 g for 10 minutes at 4°C. The protein pellet was washed with 1 ml of 1 M Tris-base, resuspended in 50 μl of 5% SDS and boiled; the concentration of proteins was measured in the supernatant by using the detergent-compatible Pierce BCA Protein Assay Kit. In each lane, 50 μg of proteins were run on 12% SDS-PAGE gels [51] and then transferred onto a nitrocellulose membrane using an iBlot2 Gel Transfer Device from Thermo Fisher Scientific and analyzed by western blotting with antibodies against Ade13 (provided by Benoit Pinson, Bordeaux, France) at a 1/50000 dilution and Cox2 (purchased from Abcam, 110 271) at a 1/500 dilution. Peroxidase labeled secondary antibodies (at a 1/10000 dilution) and the ECL reagent of Amersham International were used to detect the Ade13 and Cox2 antibody conjugates.

Human cell culture and assays with DSF

MELAS cybrids. The SH-SY5Y WT and mutant neuronal cybrid cells carrying the m.3243A > G Mitochondrial Encephalomyopathy, Lactic Acidosis, Stroke-like episodes (MELAS) mutation with a heteroplasmic state of 98.6% were cultured in DMEM high glucose (HG, 4.5 g/l) medium (Pan biotech) supplemented with 10% fetal bovine serum (FBS, Gibco), 1% glutamine and 50 μg/ml uridine (Sigma) and 100 μg/ml sodium pyruvate (Gibco) at 37°C with 5% CO_2 in a humidified atmosphere as described before [33]. To test the influence of DSF, patient and control cybrids cells were cultured during one week in DMEM medium containing a very low glucose concentration (VLG, 0.5 g/l) without uridine and pyruvate, and changed every two days, and were then exposed for 48 h to different concentrations of DSF (freshly dissolved in DMSO).

Barth syndrome cells. Eight Barth syndrome (BTHS) patient fibroblasts and two from healthy individuals (controls) were cultured like SH-SY5Y cells except that the HG DMEM medium was from Gibco. To test the influence of DSF, patient and control fibroblasts were cultured in low glucose (LG, 1 g/l) DMEM medium and exposed for 96 h to different concentrations of DSF (freshly dissolved in DMSO).

One BTHS patient myoblast line and one control cell line from a healthy individual were cultured in Skeletal Muscle Cell Basal medium (SMCM from PromoCell) at 37°C with 5% CO_2 in a humidified atmosphere. To test the influence of DSF, patient and control myoblasts were cultured in the same medium and exposed for 120 h to different concentrations of DSF (dissolved in DMSO).

Human cell proliferation rate measurement

Proliferation rate of human cells was measured in LG medium (to metabolically force the cells to rely on OXPHOS rather than glycolysis) using the Sulforhodamine B (SRB) staining protocol described in [52]. Briefly, freshly grown cells were seeded in 384-well plates and incubated for 8 h at 37°C in a humidified atmosphere with 5% CO_2. They were then exposed to different concentrations (each in triplicate) of DSF freshly dissolved in DMSO. After 96 h or 120 h of incubation (for fibroblasts or myoblasts respectively), the cells were fixed to a plastic substratum with trichloroaceticacid and stained with sulforhodamineB dye in 1% aqueous acetic acid. After elimination of the dye in excess, the bound part was solubilized with Tris base at pH 10 and evaluated by optical density (OD) at 515 nm using an ELISA plate reader. The average data from three independent experiments are expressed in percentage relative to the controls. Growth is calculated as [OD (cells + DSF) − OD (Day 0 cells)]/[OD (cells + DMSO) − OD (Day 0 cells)].

Oxygen consumption of human cells

The respiratory rates of 3–5 × 10^6 cells were recorded at 37°C in 2-ml glass chambers using a high-resolution Oxygraph respirometer (Oroboros, Innsbruck, Austria). 0.5 μl of oligomycin (Sigma, O4876) at a concentration of 4 mg/ml was injected to visualize respiration under non-phosphorylating conditions, which is not coupled to ATP synthesis; increasing concentrations of carbonyl cyanide p-(trifluoromethoxy) phenylhydrazone FCCP (Sigma, C2759) from 100 nM to 300 nM were then added to observe the maximal respiratory capacity under uncoupled conditions; finally, 4 μl of antimycin A (Sigma, A8674) at a concentration of 1 mg/ml was injected to assess non-mitochondrial respiration. For normalization, three aliquots of 500 μl of cells suspension was removed and its protein content was measured using the detergent-compatible Pierce BCA Protein Assay Kit.

Western blot on human protein extracts

The JESS Simple Western-Blots (ProteinSimple®, Bio-Techne, Minneapolis, MN, USA) were performed using dry cell pellets from SH-SY5Y cells. The samples were resuspended in 1X RIPA buffer + protease inhibitors at a ratio of 15 μl per million cells. The

samples were then placed on a rotating plate in a cold chamber for 15 minutes. A centrifugation step at 14000 g for 15 minutes at 4°C was required to collect the soluble proteins contained in the supernatant, followed by a 1:20 dilution with NaCl. Protein quantification was performed using the BCA kit to determine the protein concentration of each sample. To analyze the lysates on the JESS instrument, samples and antibodies were first tested at different concentrations (2, 0.4, and 0.08 mg/ml for samples and 1:10, 1:50, and 1:250 for antibodies, respectively) to optimize the results. The samples at 2 mg/ml and 0.08 mg/ml (for COX2 and SOD1, respectively) were diluted in 0.1X Sample Buffer and 1X fluorescent master mix (EZ standard pack I; ProteinSimple®), and 3 μl were loaded per well. COX2 antibody and the SOD1 antibody were used at 1:50, diluted in antibody diluent without milk (Bio-Techne), and added at 5 μl per well. Tubulin and TOMM20 antibodies were used at 1:50 as loading controls. The secondary antibody (HRP anti-rabbit, HRP anti-mouse, and NIR anti-mouse) and chemiluminescent reagents were used according to the kit instructions (anti-rabbit chemiluminescence detection module; ProteinSimple®, Bio-Techne). The reagents, plates, and capillary cartridges used were from the 12–230 kDa separation module (ProteinSimple®, Bio-Techne).

Mitochondrial copper measurement

To determine the mitochondrial copper content, mitochondrial fraction from the SH-SY5Y WT and mutant cybrid cells carrying the m.3243A > G MELAS mutation, exposed to 10 nM DSF or vehicle alone during 48 h, were enriched by differential centrifugation as described elsewhere [53]. Mitochondrial copper content in WT and mutant cells was evaluated using inductively coupled plasma-mass spectrometry (ICP- MS) (7800, Agilent technologies, Santa Clara, USA). The samples were mineralized using nitric acid (Suprapur, Merck, Darmstadt, Allemagne) at 70°C and then diluted 20 times with 0.5% nitric solution containing the internal standard (rhodium (^{103}Rh, E1V:7.46 eV) (1 g/l, Agilent technologies, Santa Clara, USA). The calibration was prepared using a copper standard solution (1 g/l, Agilent technologies, Santa Clara, USA) and ranged from 2.5 to 800 μg/l. To avoid polyatomic interference, helium was used as collision gas and the ^{65}Cu isotope was chosen. Internal quality controls (5, 12.5, 180 and 360 μg/l) were used. The method was validated according to manufacturer's recommendations with a limit of quantification (2.5 μg/l) and a coefficient variation < 20%, intra- and inter-day precisions.

Statistical tests.

Statistical analyses were performed using the software GraphPad Prism. The data are the means ± SEM of at least three independent experiments and statistical significance of variations among samples was estimated with two-way ANOVA, using Bonferroni multiple comparison or Tukey Anova multifactorial test (*P value < 0.05; **P < 0.01; ***P < 0.001; ****P < 0.0001).

Acknowledgements and Funding

This work was supported by AFM-Téléthon (Association Française contre les Myopathies) Research Project number: 17122 to GD, MB, AR, AD, VPr, and DTT and 22931 to VPa, SA, NB, AD, VPr and DTT. CA and DTT gratefully acknowledge Dr Jean-Paul di Rago for his constant support, discussions and help in preparing the manuscript. We thank very much Pascale de Lonlay for sending us myoblasts from Barth patients and healthy individuals and Alexa Bourand-Plantefol for technical help. We thank Karine Rottier for her work and support to the Mitodrug project.

In memoriam of Dr Agnès Delahodde who passed away during the study.

Supplementary data

Supplementary data is available at *HMG Journal* online.

Conflict of interest statement: The authors declare no conflict of interest.

References

1. Skladal D, Halliday J, Thorburn DR. Minimum birth prevalence of mitochondrial respiratory chain disorders in children. *Brain* 2003;**126**:1905–1912.
2. DiMauro S, Schon EA. Mitochondrial respiratory-chain diseases. *N Engl J Med* 2003;**348**:2656–2668.
3. Vafai SB, Mootha VK. Mitochondrial disorders as windows into an ancient organelle. *Nature* 2012;**491**:374–383.
4. Zeviani M, Carelli V. Mitochondrial disorders. *Curr Opin Neurol* 2007;**20**:564–571.
5. Murphy MP, Hartley RC. Mitochondria as a therapeutic target for common pathologies. *Nat Rev Drug Discov* 2018;**17**:865–886.
6. Zong Y, Li H, Liao P. *et al.* Mitochondrial dysfunction: mechanisms and advances in therapy. *Signal Transduct Target Ther* 2024;**9**:124.
7. Kumar S, Roy V. Repurposing drugs: an empowering approach to drug discovery and development. *Drug Res (Stuttg)* 2023;**73**: 481–490.
8. Lasserre JP, Dautant A, Aiyar RS. *et al.* Yeast as a system for modeling mitochondrial disease mechanisms and discovering therapies. *Dis Model Mech* 2015;**8**:509–526.
9. Bonnefoy, N. and Fox, T.D. (2001) Genetic transformation of Saccharomyces cerevisiae mitochondria. *Methods Cell Biol*, **65**, 381–396, New York, Elsevier.
10. Couplan E, Aiyar RS, Kucharczyk R. *et al.* A yeast-based assay identifies drugs active against human mitochondrial disorders. *Proc Natl Acad Sci USA* 2011;**108**:11989–11994.
11. Taffin de Tilques M, Lasserre JP, Godard F. *et al.* Decreasing cytosolic translation is beneficial to yeast and human Tafazzin-deficient cells. *Microb Cell* 2018;**5**:220–232.
12. Laleve A, Panozzo C, Kuhl I. *et al.* Artemisinin and its derivatives target mitochondrial c-type cytochromes in yeast and human cells. *Biochim Biophys Acta Mol Cell Res* 2020;**1867**:118661.
13. Banys P. The clinical use of disulfiram (Antabuse): a review. *J Psychoactive Drugs* 1988;**20**:243–261.
14. Jacobsen E, Martensen-Larsen O. Treatment of alcoholism with tetraethylthiuram disulfide (antabuse). *JAMA J Am Med Assoc* 1949;**139**:918–922.
15. Zeng M, Wu B, Wei W. *et al.* Disulfiram: a novel repurposed drug for cancer therapy. *Chin Med J* 2024;**137**:1389–1398.
16. Bach S, Talarek N, Andrieu T. *et al.* Isolation of drugs active against mammalian prions using a yeast-based screening assay. *Nat Biotechnol* 2003;**21**:1075–1081.
17. De Luca C, Zhou Y, Montanari A. *et al.* Can yeast be used to study mitochondrial diseases? Biolistic tRNA mutants for the analysis of mechanisms and suppressors. *Mitochondrion* 2009;**9**: 408–417.
18. Bonnefoy N, Bsat N, Fox TD. Mitochondrial translation of Saccharomyces cerevisiae COX2 mRNA is controlled by the nucleotide sequence specifying the pre-Cox2p leader peptide. *Mol Cell Biol* 2001;**21**:2359–2372.
19. Baruffini E, Lodi T, Dallabona C. *et al.* Genetic and chemical rescue of the Saccharomyces cerevisiae phenotype induced by

mitochondrial DNA polymerase mutations associated with progressive external ophthalmoplegia in humans. *Hum Mol Genet* 2006;**15**:2846–2855.
20. Ostojic J, Panozzo C, Lasserre JP. *et al.* The energetic state of mitochondria modulates complex III biogenesis through the ATP-dependent activity of Bcs1. *Cell Metab* 2013;**18**:567–577.
21. Taffin de Tilques M, Tribouillard-Tanvier D, Tetaud E. *et al.* Overexpression of mitochondrial oxodicarboxylate carrier (ODC1) preserves oxidative phosphorylation in a yeast model of Barth syndrome. *Dis Model Mech* 2017;**10**:439–450.
22. Lefebvre-Legendre L, Vaillier J, Benabdelhak H. *et al.* Identification of a nuclear gene (FMC1) required for the assembly/stability of yeast mitochondrial F(1)-ATPase in heat stress conditions. *J Biol Chem* 2001;**276**:6789–6796.
23. Schwimmer C, Lefebvre-Legendre L, Rak M. *et al.* Increasing mitochondrial substrate-level phosphorylation can rescue respiratory growth of an ATP synthase-deficient yeast. *J Biol Chem* 2005;**280**:30751–30759.
24. Deitrich RA, Erwin VG. Mechanism of the inhibition of aldehyde dehydrogenase in vivo by disulfiram and diethyldithiocarbamate. *Mol Pharmacol* 1971;**7**:301–307.
25. Lehner T, Gao B, Mackowiak B. Alcohol metabolism in alcohol use disorder: a potential therapeutic target. *Alcohol Alcohol* 2024;**59**:1–8.
26. Allensworth JL, Evans MK, Bertucci F. *et al.* Disulfiram (DSF) acts as a copper ionophore to induce copper-dependent oxidative stress and mediate anti-tumor efficacy in inflammatory breast cancer. *Mol Oncol* 2015;**9**:1155–1168.
27. Nagai M, Vo NH, Shin Ogawa L. *et al.* The oncology drug elesclomol selectively transports copper to the mitochondria to induce oxidative stress in cancer cells. *Free Radic Biol Med* 2012;**52**:2142–2150.
28. Zheng P, Zhou C, Lu L. *et al.* Elesclomol: a copper ionophore targeting mitochondrial metabolism for cancer therapy. *J Exp Clin Cancer Res* 2022;**41**:271.
29. Takahashi Y, Kako K, Kashiwabara S. *et al.* Mammalian copper chaperone Cox17p has an essential role in activation of cytochrome C oxidase and embryonic development. *Mol Cell Biol* 2002;**22**:7614–7621.
30. Morrison BW, Doudican NA, Patel KR. *et al.* Disulfiram induces copper-dependent stimulation of reactive oxygen species and activation of the extrinsic apoptotic pathway in melanoma. *Melanoma Res* 2010;**20**:11–20.
31. Bouchez C, Devin A. Mitochondrial biogenesis and mitochondrial reactive oxygen species (ROS): a complex relationship regulated by the cAMP/PKA Signaling pathway. *Cells* 2019;**8**:287.
32. Yoboue ED, Mougeolle A, Kaiser L. *et al.* The role of mitochondrial biogenesis and ROS in the control of energy supply in proliferating cells. *Biochim Biophys Acta* 2014;**1837**:1093–1098.
33. Desquiret-Dumas V, Gueguen N, Barth M. *et al.* Metabolically induced heteroplasmy shifting and l-arginine treatment reduce the energetic defect in a neuronal-like model of MELAS. *Biochim Biophys Acta* 2012;**1822**:1019–1029.
34. Trist BG, Hilton JB, Hare DJ. *et al.* Superoxide dismutase 1 in health and disease: how a frontline antioxidant becomes neurotoxic. *Angew Chem Int Ed Engl* 2021;**60**:9215–9246.
35. Kwolek-Mirek M, Zadrag-Tecza R, Bartosz G. Ascorbate and thiol antioxidants abolish sensitivity of yeast Saccharomyces cerevisiae to disulfiram. *Cell Biol Toxicol* 2012;**28**:1–9.
36. Xu Y, Lu L, Luo J. *et al.* Disulfiram alone functions as a Radiosensitizer for pancreatic cancer both In vitro and In vivo. *Front Oncol* 2021;**11**:683695.
37. Shah, O'Brien P, Xi Y, Miller JR. *et al.* Disulfiram (Antabuse) activates ROS-dependent ER stress and apoptosis in oral cavity squamous cell carcinoma. *J Clin Med* 2019;**8**:611.
38. Nyvltova E, Dietz JV, Seravalli J. *et al.* Coordination of metal center biogenesis in human cytochrome c oxidase. *Nat Commun* 2022;**13**:3615.
39. Soma S, Morgada MN, Naik MT. *et al.* COA6 is structurally tuned to function as a thiol-Disulfide oxidoreductase in copper delivery to mitochondrial cytochrome c oxidase. *Cell Rep* 2019;**29**:4114–4126.e5.
40. Soma S, Latimer AJ, Chun H. *et al.* Elesclomol restores mitochondrial function in genetic models of copper deficiency. *Proc Natl Acad Sci USA* 2018;**115**:8161–8166.
41. Guthrie LM, Soma S, Yuan S. *et al.* Elesclomol alleviates Menkes pathology and mortality by escorting Cu to cuproenzymes in mice. *Science* 2020;**368**:620–625.
42. Barrientos A, Zambrano A, Tzagoloff A. Mss51p and Cox14p jointly regulate mitochondrial Cox1p expression in Saccharomyces cerevisiae. *EMBO J* 2004;**23**:3472–3482.
43. Su X, Rak M, Tetaud E. *et al.* Deregulating mitochondrial metabolite and ion transport has beneficial effects in yeast and human cellular models for NARP syndrome. *Hum Mol Genet* 2019;**28**:3792–3804.
44. Rak M, Tetaud E, Godard F. *et al.* Yeast cells lacking the mitochondrial gene encoding the ATP synthase subunit 6 exhibit a selective loss of complex IV and unusual mitochondrial morphology. *J Biol Chem* 2007;**282**:10853–10864.
45. Soto IC, Fontanesi F, Valledor M. *et al.* Synthesis of cytochrome c oxidase subunit 1 is translationally downregulated in the absence of functional F1F0-ATP synthase. *Biochim Biophys Acta* 2009;**1793**:1776–1786.
46. Fontanesi F, Jin C, Tzagoloff A. *et al.* Transcriptional activators HAP/NF-Y rescue a cytochrome c oxidase defect in yeast and human cells. *Hum Mol Genet* 2008;**17**:775–788.
47. Lutsenko S, Roy S, Tsvetkov P. Mammalian copper homeostasis: physiologic roles and molecular mechanisms. *Physiol Rev* 2024;**105**:441–491.
48. Zhang L, Xie A, Ma J. *et al.* Unveiling Cuproptosis: mechanistic insights, roles, and leading advances in oncology. *Biochim Biophys Acta rev. Cancer* 2024;**1879**:189180.
49. Saint-Georges Y, Bonnefoy N, di Rago JP. *et al.* A pathogenic cytochrome b mutation reveals new interactions between subunits of the mitochondrial bc1 complex. *J Biol Chem* 2002;**277**:49397–49402.
50. Minet M, Dufour ME, Lacroute F. Complementation of Saccharomyces cerevisiae auxotrophic mutants by Arabidopsis thaliana cDNAs. *Plant J* 1992;**2**:417–422.
51. Laemmli UK. Cleavage of structural proteins during the assembly of the head of bacteriophage T4. *Nature* 1970;**227**:680–685.
52. van Tonder A, Joubert AM, Cromarty AD. Limitations of the 3-(4,5-dimethylthiazol-2-yl)-2,5-diphenyl-2H-tetrazolium bromide (MTT) assay when compared to three commonly used cell enumeration assays. *BMC Res Notes* 2015;**8**:47.
53. Bonnet C, Augustin S, Ellouze S. *et al.* The optimized allotopic expression of ND1 or ND4 genes restores respiratory chain complex I activity in fibroblasts harboring mutations in these genes. *Biochim Biophys Acta* 2008;**1783**:1707–1717.